N.m.r. and molecular-modelling studies of the solution conformation of heparin

Barbara MULLOY,*‡ Mark J. FORSTER,* Christopher JONES* and David B. DAVIES†

*National Institute for Biological Standards and Control, Blanche Lane, South Mimms, Potters Bar, Herts. EN6 3QG,
†Department of Chemistry, Birkbeck College, Gordon House, 29 Gordon Square, London WC1H 0PP, U.K.

The solution conformations of heparin and de-N-sulphated, re-N-acetylated heparin have been determined by a combination of n.m.r. spectroscopic and molecular-modelling techniques. The ^1H- and ^{13}C-n.m.r. spectra of these polysaccharides have been assigned. Observed ^1H–^1H nuclear Overhauser enhancements (n.O.e.s) have been simulated using the program NOEMOL [Forster, Jones and Mulloy (1989) J. Mol. Graph. 7, 196–201] for molecular models derived from conformational-energy calculations; correlation times for the simulations were chosen to fit experimentally determined ^{13}C spin-lattice relaxation times. In order to achieve good agreement between calculated and observed ^1H–^1H n.O.e.s it was necessary to assume that the reorientational motion of the polysaccharide molecules was not isotropic, but was that of a symmetric top. The resulting model of heparin in solution is similar to that determined in the fibrous state by X-ray-diffraction techniques [Nieduszynski, Gardner and Atkins (1977) Am. Chem. Soc. Symp. Ser. **48**, 73–80].

INTRODUCTION

The glycosaminoglycan heparin has been in clinical use for many years as an antithrombotic and anticoagulant agent. It has recently attracted attention in other contexts, notably that of stabilization and potentiation of fibroblast growth factors (FGFs) (Gospodarowicz and Cheng, 1986; Damon et al., 1989). Its close structural relative heparan sulphate is a ubiquitous component of the cell surface and has been shown to be an essential part of receptor complexes for growth factors (Yayon et al., 1991; Rapraeger et al., 1991) and for some viruses (Savitsky et al., 1990). Description of the structures and structure–function relationships of both compounds at the molecular level will rationalize and simplify the processes of standardization and control in respect of both current and future clinical applications.

Both heparin and heparan sulphate exert their effects by modulating the activity of proteins to which they bind. As structures for heparin-binding proteins become available, there is an increasing number of molecular-modelling studies of protein–heparin interactions. Such studies need molecular models of heparin. For the heparin polysaccharide, the best data available are given by solid-state-diffraction studies of heparin fibres (Nieduszynski et al., 1977). Solution-state structures, determined by n.m.r. spectroscopy, are only available for synthetic oligosaccharides resembling the sequence in heparin which has high affinity for antithrombin (Ragazzi et al., 1990). The interaction of antithrombin with the high-affinity sequence has been modelled (Grootenhuis and van Boeckel, 1991). Molecular-modelling studies of protein interactions with the heparin polysaccharide have used the fibrous structure (e.g. Cowan et al., 1986) or models based on energy calculations alone (Cardin et al., 1991).

We report the characterization by n.m.r. methods of the solution conformation of the main repeating structure in the heparin polysaccharide (1) and that in N-desulphated re-N-acetylated heparin (2), using inter-residue nuclear Overhauser enhancements (n.O.e.s) to characterize torsional angles round glycosidic bonds, and coupling-constant data, where available, to determine the orientation of exocyclic groups [at C-6 and C-2 of α-D-glucosamine (GlcN) residues]. We have used the program NOEMOL (Forster et al., 1989) to simulate n.O.e.s for molecular models of dodecasaccharides corresponding to the polysaccharides, using conformational-energy calculations of an unsophisticated kind to generate the initial models. As found previously (Forster et al., 1989) it was necessary to use a symmetric-top model for overall molecular reorientation in solution in order to achieve good agreement between calculated and observed inter- and intra-residue n.O.e.s.

The conformation of iduronate-containing polysaccharides and oligosaccharides is complicated by the well-documented conformational mobility of the iduronate pyranose ring. When the α-L-iduronic acid (IdoA) residue is at the reducing end of an oligosaccharide, n.m.r. data have been interpreted in terms of contributions from three conformers, the $^4C_1$ and $^1C_4$ chairs and the $^2S_0$ skew-boat (Figure 1) (Sanderson et al., 1987). When the IdoA residue is internal, only two conformations, the $^1C_4$ chair and the $^2S_0$ skew boat, are accessible (Ferro et al., 1986; van Boeckel et al., 1987a; Ferro et al., 1990). This conformational flexibility complicates interpretation of the n.m.r. data and molecular-modelling procedures. However, sulphated IdoA residues substituted at the 4-position with N-acetylglucosamine, as in 2, assume the $^1C_4$ chair conformer almost exclusively (van Boeckel et al., 1987a); 2 is therefore useful as a compound for which a single conformation can be assumed for interpretation of n.m.r. data, allowing subsequent extension of the study to include heparin (1), in which the conformation of the iduronate residue is assumed to be a dynamic equilibrium between the $^1C_4$ and $^2S_0$ forms.
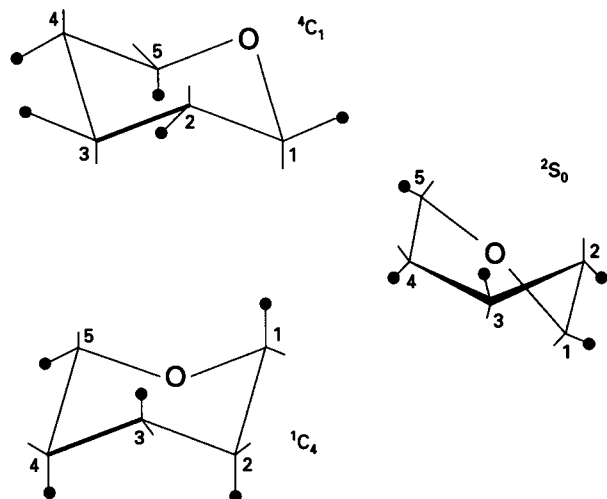
Figure 1 The three low-energy conformations of the α-L-iduronopyranose ring which are considered to be the main contributors to its conformational equilibrium in solution

● symbolizes heavy atom substituents.

MATERIALS AND METHODS

Materials

Lung heparin (**1**) was material remaining from the Second International Standard of heparin (Bangham and Mussett, 1959); N-desulphated, re-N-acetylated heparin (**2**) was prepared from lung heparin by N-desulphation (Nagasawa and Inoue, 1980), followed by re-N-acetylation (Danishevsky et al., 1960).

Molecular-mass distribution estimations by gel-permeation chromatography

Gel-permeation chromatography of the polysaccharides was performed on a 60 cm column of TSK SX 3000 (Anachem, Luton, Beds., U.K.), with 0.1 M ammonium acetate as eluant at 0.5 ml/min using refractometric detection.

Preparations of samples for n.m.r. studies

Compounds **1** and **2** were subjected to ion-exchange chromatography to remove paramagnetic impurities. A column (1 cm × 10 cm) of AG 50W-X8 (Bio-Rad, Hemel Hempstead, Herts., U.K.) was converted into the Na^+ form by treatment with 5 ml of 0.1 M NaOH and washed with water for at least 24 h before use. Samples for n.m.r. were applied to the column, eluted with about 30 ml of water, and dried by evaporation under reduced pressure. For [1]H n.m.r., 20–30 mg of each polysaccharide was freeze-dried three times from 99.8 % ^2H_2O (Goss Scientific Instruments, Ingatestone, Essex, U.K.), then dissolved in 0.6 ml of 100 % ^2H_2O (Aldrich Chemical Co., Poole, Dorset, U.K.) for n.m.r. spectroscopy in a 5 mm tube. For [13]C n.m.r., about 100 mg of each polysaccharide was dissolved in 2.5 ml of ^2H_2O for spectroscopy in a 10 mm n.m.r. tube.

N.m.r. spectroscopy

Spectra (500 MHz ^{1}H and 125 MHz ^{13}C) were recorded on Bruker AM 500 and JEOL GSX 500 spectrometers; 400 MHz [1]H

spectra and 100 MHz ^{13}C spectra were recorded on a Bruker AM 400 spectrometer; 67.5 MHz ^{13}C spectra were recorded on a Bruker WH 270, and 50 MHz ^{13}C spectra on a Bruker WM 200, spectrometer. All the spectra were recorded at elevated temperature, usually 60 °C.

[1]H n.m.r. spectra of polysaccharides in 80 % ^1H_2O/20 % ^2H_2O were recorded at 400 MHz using the $1.\overline{3}.3.\overline{1}$ sequence for water suppression (Hore, 1983).

Magnitude-mode two-dimensional correlation-spectroscopy (COSY) spectra of the polysaccharides were acquired at 500 MHz. The instrument manufacturer's standard pulse sequences were used in all cases. Typically 256 spectra of 1024 points each were used, with narrow spectral width (3–4 p.p.m.) giving digital resolution in F2 of about 2 Hz/point. Zero-filling to 512 points was used in F1, with no zero-filling in F2.

Truncated driven n.O.e.s were measured at 500 MHz from difference spectra by integration and are quoted as a percentage of the area under the irradiated resonance. In order to record n.O.e.s on protons with resonances near that of $^1HO^2H$, some measurements were made at 50 °C. The difference in n.O.e. values due to the 10 °C temperature difference was within experimental error.

[1]H/^{13}C heteronuclear correlated spectra were recorded at 400 MHz using standard pulse sequences supplied by the instrument manufacturers.

[13]C spin-lattice relaxation rates (R_1) were measured at 67.5 and 50 MHz by the inversion-recovery method. Ten spectra were obtained with a variable delay of 0.001–7.0 s; a relaxation delay of 7 s was sufficient to allow full relaxation of the ring carbon atoms, though probably insufficient for the methyl carbon atoms. Relaxation rates were calculated from the intensities in the spectra using the Marquardt algorithm for non-linear curve-fitting.

Computational methods

Molecular models were built using ChemX software (designed and distributed by Chemical Design Ltd., Oxford, U.K.) running on a MicroVax II computer. Calculations of van der Waals energies and plots of van der Waals energy against geometry were also performed using the ChemX software. Refinement of the structures by minimization of conformational energy was performed in the MM2 force field (Burkert and Allinger, 1982), modified for carbohydrates as recommended by Jeffrey and Taylor (1980). The program NOEMOL, available from the Quantum Chemistry Program Exchange (QCPE 636), Indiana University, Bloomington, IN, U.S.A. (Forster et al., 1989), was run on Sun 3/160 and IRIS 4D/310 computers.

Modelling of monosaccharides

Co-ordinates for the monosaccharide N-acetylglucosamine were obtained from the Cambridge Crystallographic Data Centre, University Chemical Laboratory, Cambridge, U.K. Co-ordinates for IdoA were obtained from crystallographic data as follows: Nieduszynski et al. (1977) for the $^1C_4$ form, Mitra et al. (1983) for the $^4C_1$ form and Chamberlain et al. (1981) for the $^2S_0$ form.

The geometry of the sulphate moieties in all the models was derived from the published crystal structure of galactose 6-sulphate (Lamba et al., 1988). In N-sulphated glucosamine, the sulphamido nitrogen atom was assumed to be tetrahedral as in the fragment $C-SO_2-NH-Csp^3$ (Allen et al., 1987); the N–S bond length was taken from the same source. Other parameters needed for the sulphate group in the MM2 force field were taken from Ragazzi et al. (1986).

Modelling of oligosaccharides

Oligosaccharides were built from monosaccharide units modelled as described above with the $C^1-O^{4'}-C^{4'}$ bond angle set to 117°, and the $C^1-O^{4'}$ and $O^{4'}-C^{4'}$ bond lengths set to 0.1398 nm (1.398 Å).
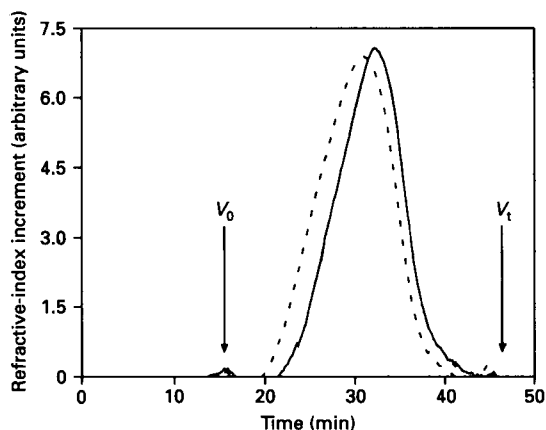
Figure 2   Gel-permeation chromatograms of 1 (——) and 2 (-----) after baseline correction

A 60 cm column of TSK SX 3000 was used, with 0.1 M ammonium acetate as eluant; the elution rate was 0.5 ml/min and refractometric detection was used. The molecular-size profiles of the two compounds are similar; 2 runs slightly faster through the column than 1, indicating that it may be a little larger.

Table 1   Proton chemical shifts and coupling constants for heparin (1) and de-N-sulphated re-N-acetylated heparin (2)

		^{1}H chemical shifts in p.p.m.†				$^3J_{H,H}$ (Hz)§	
		1	2			1	2
I*	H^1	5.22	5.14	I	H^1–H^2	2.9	< 2.0
I	H^2	4.35	4.33	I	H^2–H^3	5.9	3.9
I	H^3	4.20	4.22	I	H^3–H^4	3.7	3.3
I	H^4	4.10	4.06	I	H^4–H^5	3.0	2.9
I	H^5	4.81	4.87				
A*	H^1	5.39	5.11	A	H^1–H^2	3.6	4.0
A	H^2	3.29	4.0‡	A	H^2–H^3	10.3	–‖
A	H^3	3.67	3.73§	A	H^3–H^4	10.0	–‖
A	H^4	3.77	3.73§	A	H^4–H^5	9.6	–‖
A	H^5	4.03	4.0‡	A	H^5–H^6 pro-(S)	2.3	–‖
A	H^6 pro-(S)	4.39	4.3‡	A	H^5–H^6 pro-(R)	< 3.0	–‖
A	H^6 pro-(R)	4.27	4.3‡	A	H^6 pro-(S)– H^6 pro-(R)	–11.6¶	–‖
A	NH	7.82					
A	H^2,NH		9.4				
CH$_3$			2.04				

* I, iduronate residue; A, glucosamine residue.
† Measured at 60 °C relative to internal TSP-d$_4$.
‡ Overlapping resonances; estimate.
§ ±0.3 Hz.
‖ Not measurable due to overlapping resonances.
¶ $^2J_{H,H}$; sign not determined experimentally.

RESULTS

Molecular-mass distributions

The gel-permeation chromatograms of 1 and 2 are shown in Figure 2. It was deduced that chemical modification had not caused serious depolymerization; there is a slight apparent increase in size on modification of 1 into 2. Both compounds are polydisperse, and have molecular-mass distributions similar to those of commercial heparins, with a mean molecular mass of about 13 kDa (Johnson and Mulloy, 1976).

^{1}H and ^{13}C n.m.r. spectra

The ^{1}H n.m.r. spectra of 1 and 2 were assigned by means of COSY spectra (results not shown). For both these poly-saccharides, two spin systems could be traced from the anomeric doublets downfield of the ^{1}HO^{2}H resonance, one consisting of five spins (arising from the IdoA residue) and one consisting of seven spins (arising from the glucosamine residue). The sample of lung heparin used in the present study was chosen for its unusually high content of 1 (> 90%), and the ^{1}H spectrum confirmed its high degree of homogeneity. This homogeneity was also reflected in the spectrum of 2.

Measurement of $^3J_{H,H}$ values from the one-dimensional ^{1}H spectra of both compounds is not accurate to better than ±0.3 Hz, owing to broad lines of the spectra even at 60 °C. This difficulty applies particularly to the IdoA signals, where $^3J_{H,H}$ values are relatively small (1–6 Hz). Chemical shifts and $^3J_{H,H}$ values are listed in Table 1. Assignment of the ^{1}H spectrum of 1 was reported by Gatti et al. (1979) and the values given in Table 1 agree with this assignment.

The stereospecific assignments for H^6-pro-(S) and H^6-pro-(R) follow those given by Nishida et al. (1988). Those authors established from the spectra of several partially ^{2}H-labelled gluco-monosaccharides that the H^6 pro-(R) signal always occurred upfield of the H^6 pro-(S) signal, and had the higher $^3J_{H5,H6}$ value. In 2 the two H^6 resonances are coincident; in 1 they are separated and the upfield resonance was assigned to H^6 pro-(R). $^3J_{H,H}$ values could not be used to differentiate between H^6 pro-(R) and H^6 pro-(S) as both H^5–H^6 coupling constants are small.

Coupling constants between H^2 and NH for 2 were measured from a ^{1}H spectrum in 80% ^{1}H$_2$O/20% ^{2}H$_2$O, in which the NH doublet occurred at 7.82 p.p.m. ($^3J_{NH,H2}$ = 9.4 Hz). ^{13}C spectra of the polysaccharides were assigned by two-dimensional heteronuclear COSY, and ^{13}C chemical shifts are listed in Table 2. The ^{13}C spectrum of 1 is similar to that reported by Gatti et al. (1979).

^{13}C relaxation times

^{13}C spin-lattice relaxation rates (R_1s) for 1 and 2 were measured at both 50 and 67.5 MHz, and are listed in Table 2. R_1s for the two compounds are similar at both fields, and are lower at 67.5 MHz than at 50 MHz. None of the ring carbon atoms in either compound displays R_1s sufficiently different from the others to be structurally significant. Relaxation rates for C^{6}s of the IdoA residues, with two attached protons, are approximately twice those of the ring carbon atoms, which have one attached proton; this implies that the rate of rotation round the C^5–C^6 bond is not more rapid than that of overall reorientation, as rapid rotation would reduce R_1 for C^6.

^{1}H–^{1}H n.O.e.s

n.O.e.s from resolved resonances in the spectra were measured by one-dimensional difference spectroscopy; inter-residue and

Table 2 ¹³C chemical shifts, and spin-lattice relaxation rates (R₁s) at 50 and 67.5 MHz, of heparin (1) and de-N-sulphated re-N-acetylated heparin (2)*†

		Chemical shift (p.p.m.)	R_1 (s⁻¹) at:	
			50 MHz‡	67.5 MHz‡
1	I C¹	102.2	5.3±0.4	4.9±0.3
	I C²	79.0	6.1±0.3‖	4.8±0.1
	I C³	72.2	6.9±0.5	4.7±0.1
	I C⁴	79.1	6.1±0.3‖	4.8±0.1
	I C⁵	72.0	6.8±0.3¶	4.8±0.1
	I C⁶	177.1	n.d.**	n.d.
	A C¹	99.6	5.7±0.4	5.0±0.2
	A C²	60.8	7.3±0.7	5.1±0.1
	A C³	72.9	7.0±0.4	4.8±0.1
	A C⁴	79.1	6.1±0.3‖	4.8±0.1
	A C⁵	72.0	6.8±0.3¶	5.0±0.2
	A C⁶	69.3	13.1±1.3	8.1±0.2
2	I C¹	100.7	5.8±0.2	4.5±0.2
	I C²	75.3	6.8±0.4	5.2±0.3
	I C³	66.0	6.3±0.3	5.8±0.4
	I C⁴	72.8	5.4±0.3	4.3±0.3
	I C⁵	69.2	6.5±0.4	4.2±0.2
	I C⁶	176.5§	n.d.	n.d.
	A C¹	95.08	6.5±0.3	5.3±0.3
	A C²	54.57	6.5±0.4	5.2±0.2
	A C³	71.30	6.3±0.3	5.2±0.2
	A C⁴	77.81	6.8±0.3	4.4±0.3
	A C⁵	70.58	6.5±0.3	5.2±0.3
	A C⁶	67.68	12.0±0.5	8.0±0.5
	C=O	176.70§		
	ACH₃	23.20	1.9±0.2	n.d.

* Measured in ²H₂O solution at 60 °C; chemical shifts are relative to internal TSP-d₄ (TSP-d₄ is at −1.94 p.p.m. relative to dioxan at 67.4 p.p.m.).
† I, iduronate residue; A, glucosamine residue.
‡ The errors shown are S.D. values.
§ Assignments may be interchanged.
‖ Coincident resonances.
¶ Coincident resonances.
** n.d., not determined.

H¹–H² n.O.e.s are shown in Tables 3 and 4 for 2 and 1 respectively. The magnitudes of n.O.e.s measured by integration of the one-dimensional difference spectra were sensitive to the presence of paramagnetic impurities; n.O.e.s apparently increased after their removal, as a result of improved lineshape enabling more accurate integration. This accounts for the difference in measured n.O.e.s between the values for 2 shown in Table 3 and those given in Forster et al. (1989) for the same compound. All measured n.O.e.s were negative in sign.

Computation of conformational energies

Conformational-energy calculations for the disaccharides, modelled as described above, were performed after adjustment of the dispositions of substituent groups to agree with n.m.r. results, particularly for the N-acetyl and hydroxymethyl groups.

The measured ³$J_{NH,CH2}$ value for 2 (9.4 Hz), is similar to ³$J_{NH,CH2}$ values in N-acetylglucosamine-containing oligosaccharides (Rao et al., 1985), which were interpreted as indicating a dihedral angle for H²–C²–N–H of about 180°. The dihedral angle H²–C²–N–H in the molecular models of N-acetylglucosamine was therefore set to this value.

Table 3 Comparison of calculated and experimental ¹H–¹H n.O.e.s and ¹³C R₁s for de-N-sulphated re-N-acetylated heparin (2)

(i) ¹H–¹H n.O.e.s (%) at 60 °C

	n.O.e. (%)		Calculated ¹C₄
	Experimental*		
	Mean	Range	
H¹A† to H³I	−34	(30.1–38.0)	−42
H⁴I	−4	(−4.1–4.6)	−2
H²A	−29	(−27.8–30.1)	−38
H¹I to H⁶ pro-(S)A	−15‡	(−13.7–15.7)	−16
H⁶ pro-(R)A			−8
H⁴A	−7	(−6.2–8.0)	−5
H²I	−7	(6.4–7.5)	−7

(ii) ¹³C R₁s

	¹³C R_1 (s⁻¹) at:			
	50 MHz (s⁻¹)		67.5 MHz	
	Exp.	Calc. ¹C₄	Exp.	Calc. ¹C₄
C¹I	5.8	5.2	4.5	4.2
C²I	6.8	8.0	5.2	6.1
C³I	6.3	5.4	5.8	4.5
C⁴I	5.4	5.3	4.3	4.4
C⁵I	6.5	8.0	4.2	6.3
C¹A	6.5	6.9	5.3	5.8
C²A	6.5	6.8	5.2	5.7
C³A	6.3	6.2	5.2	5.2
C⁴A	6.8	7.1	4.4	5.9
C⁵A	6.5	6.8	5.2	5.7
C⁶A	12.0	14.2	8.0	10.9

(iii) Glycosidic torsional angles used for calculated n.O.e.s

	¹C₄ angle (°)	
	ϕ_H	ψ_H
AI	−68	−40
IA	41	14

* Truncated driven n.O.e.s; spins saturated for 200 ms, measured at 500 MHz in ²H₂O. Values shown are the means of four measurements.
† A, glucosamine; I, iduronate.
‡ H⁶ pro-(R) and H⁶ pro-(S) signals are coincident.

³$J_{H5,H6}$ values could be measured for 1 but not 2, where the H⁶ signals were coincident. The small, and nearly equal, values for ³$J_{H5,H6proS}$ and ³$J_{H5,H6proR}$ in heparin have been interpreted as indicating a preponderance of the g,g rotamer, O⁶–C⁶–C⁵–H⁵ = 180° (Gatti et al., 1979), and the same conclusion has been drawn for 6-O-sulphated glucosamine in a synthetic heparin oligosaccharide (Ragazzi et al., 1990). The C⁵–C⁶ bond was given the g,g conformer in the glucosamine residues of both polysaccharides.

Disaccharides: conformational-energy calculations

Four disaccharide models were produced for both 1 and 2: GlcN-(1-4)-IdoA (A–I linkage) and IdoA-(1-4)-GlcN (I–A linkage), with iduronate in both the ¹C₄ and ²S₀ forms.

Table 4 Comparison of calculated and experimental ^{1}H–^{1}H n.O.e.s and ^{13}C R_1s for heparin (1)

(i) ^{1}H–^{1}H n.O.e.s at 500 MHz, 50 °C

| | n.O.e. (%) | | | |
| | (a) Experimental* | | (b) Calculated | |
	Mean	Range	^{1}C$_4$	^{2}S$_0$
H^{1}A† to H^{3}I	−12	(−11.2–13.5)	−24	−1
H^{4}I	−12	(−11.7–13.2)	−4	−20
H^{2}A	−29	(−26.9–32.9)	−24	−12
H^{1}I to H^6 pro-(S)A	−11	(−10.0–11.1)	−6	−12
H^6 pro-(R)A	−5	(−4.8–5.4)	−2	−1
H^{4}A	−6	(−5.3–6.1)	−2	−2
H^{2}I	−5	(−5.8–6.2)	−6	−2

(ii) ^{13}C R_1s

	^{13}C R_1 (s^{-1}) at:					
	50 MHz			67.5 MHz		
		Calculated			Calculated	
	Exp.	^{1}C$_4$	^{2}S$_0$	Exp.	^{1}C$_4$	^{2}S$_0$
C^{1}I	5.3	4.9	5.0	4.9	4.0	4.1
C^{2}I	6.1	7.9	6.9	4.8	6.3	5.7
C^{3}I	6.9	5.7	6.9	4.7	4.9	5.8
C^{4}I	6.1	4.9	4.7	4.8	3.9	3.8
C^{5}I	6.8	7.9	7.9	4.8	5.8	6.1
C^{1}A	5.7	7.0	5.8	5.0	5.8	4.8
C^{2}A	7.3	6.9	7.9	5.1	5.8	6.3
C^{3}A	7.0	6.4	7.5	4.8	5.4	6.3
C^{4}A	6.1	7.2	7.9	4.8	5.9	6.3
C^{5}A	6.8	7.0	7.9	5.0	5.9	6.3
C^{6}A	13.1	14.9	13.6	8.1	11.8	11.2

(iii) Glycosidic torsional angles for calculated values

| | Angle (°) | | | |
| | ^{1}C$_4$ | | ^{2}S$_0$ | |
	ϕ_H	ψ_H	ϕ_H	ψ_H
AI	−39	−33	−9	−41
IA	41	14	61	16

* Truncated driven n.O.e.s; spins saturated for 200 ms, measured at 500 MHz in ^{2}H$_2$O. Values given are the means of four measurements.

† I, iduronate; A, glucosamine.

By using the ChemX program, both dihedral angles (ϕ_H: H^1–C^1–O$^{4'}$–C$^{4'}$; ϕ_H = 0 when the bonds H^1–C^1 and O$^{4'}$–C$^{4'}$ are eclipsed; and ψ_H: C^1–O$^{4'}$–C$^{4'}$–H$^{4'}$; ψ_H = 0 when the C^1–O$^{4'}$ and C$^{4'}$–H$^{4'}$ bonds are eclipsed) were varied over the full range possible (−180° to +180°) and non-bonded energy was calculated at 20^c intervals in a grid search. For each grid point, ten cycles of energy minimization, allowing rotation of all exocyclic bonds, was carried out.

Conformations corresponding to energy minima in the maps were refined by energy minimization in the MM2 force field. This allowed alteration of bond lengths and angles, as well as rotation about bonds, and the calculated energy includes terms other than non-bonded interactions between atoms. MM2 minimization included the two glycosidic bond torsional angles, and allowed minimum energy conformations between the 20° steps of the systematic search to be located. The resulting models do not necessarily correspond to the structures which would have resulted from a systematic search of the whole conformational space using MM2 minimization at each step, as has been recommended (French, 1988). The results of the non-bonded energy calculations are shown as contour maps in Figure 3. The absolute values of the non-bonded energies are not presented, as they have little physical meaning, and the purpose of the exercise is to identify conformations in which steric clashes are avoided, to act as starting structures for later refinement against experimental data.

A–I linkages

When IdoA is set in the ^{1}C$_4$ form, energy minima for the A–I linkages are seen in the lower left-hand quadrant of the maps in Figure 3(a). In both compounds, alteration of the ring conformation to the ^{2}S$_0$ form (Figure 3b) reduces the area of the map within 83.7 kJ (20 kcal) of the minimum. Values of ϕ_H and ψ_H for MM2 minima are shown in Table 5.

I–A linkages

The energy maps for the I–A linkages of 1 and 2 show a large area of relatively low energy (Figures 3c and 3d) with two or more poorly defined minima: one with both ϕ_H and ψ_H positive, and a second with ϕ_H negative, and ψ_H small and positive or small and negative. For 2, a second minor area of low energy exists at ϕ_H = 0°, ψ_H = 180°. Differences between the maps with iduronate in the ^{1}C$_4$ and ^{2}S$_0$ (Figures 3c and 3d respectively) forms are not great; in every case the areas of low energy for the two forms overlap almost entirely. The maps shown are calculated for the g,g rotamer of the C^5–C^6 bonds in the glucosamine residues; a similar set of maps was prepared for 2 with the g,t rotamer (O^6–C^6–C^5–H^5 = −60°, but these are not shown as they do not differ significantly from the maps with the g,g rotamer.

MM2 calculations for the disaccharide models did not provide clear global minima; the two minima in the maps were almost equienergetic in the MM2 force field. Conformations corresponding to these minima are listed in Table 5. On the basis of these glycosidic angles, dodecasaccharide models (two for each compound, with the IdoA residue set in the ^{1}C$_4$ and ^{2}S$_0$ forms) were built for use in n.O.e. simulations.

n.O.e. simulations using the program NOEMOL

The program NOEMOL (Forster et al., 1989) takes the Cartesian co-ordinates of a molecular model, and, given the field of the spectrometer and the correlation time to be used, calculates the full relaxation matrix of cross- and auto-relaxation rate constants for all proton–proton interactions. For a particular proton (or group of protons), the n.O.e.s to other spins resulting from a defined set of experimental conditions (for example, saturation or inversion of the chosen spin or spins) can then be calculated over a given time course. In this way spin diffusion is automatically allowed for, which is particularly important for the interpretation of n.O.e.s for macromolecules. n.O.e. simulations for the two polysaccharides corresponded to the experimental conditions under which the n.O.e.s had been measured. As the experiments had been performed for ^{2}H$_2$O solutions of the polysaccharides, the dodecasaccharide models described above

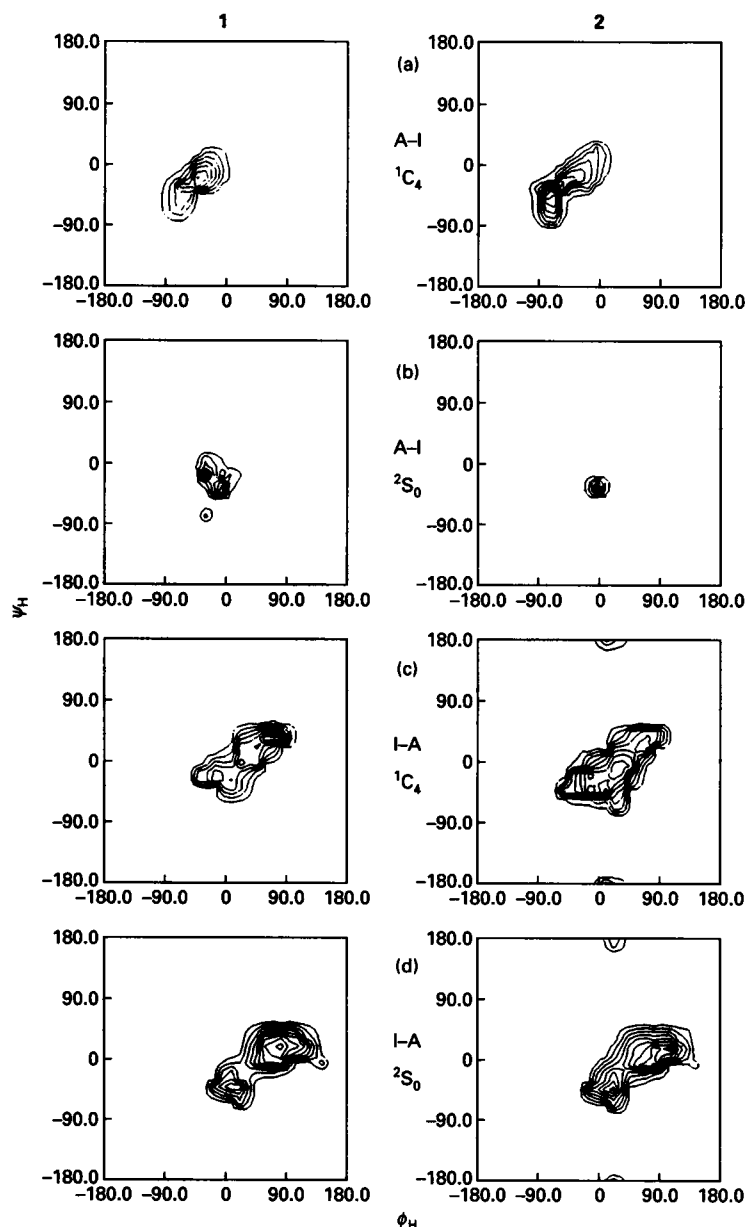**Figure 3   Contour plots of van der Waals energy [2 kcal/mol (1 kcal ≡ 4.184 kJ) between contours] against ϕ_H and ψ_H for 1 (heparin) and 2, calculated as described in the text**

(a) the A–I disaccharide with the IdoA residue in the $^1C_4$ conformation; (b) the A–I disaccharide in the $^2S_0$ conformation; (c) the I–A disaccharide with the IdoA residue in the $^1C_4$ conformation; and (d) the I–A disaccharide with the IdoA residue in the $^2S_0$ conformation (I, iduronate; A, glucosamine).

were prepared for NOEMOL by 'deuteriating' them; that is to say, the atom names of exchangeable hydrogen atoms in the data files were altered to exclude them from the relaxation matrix.

Choice of correlation time: isotropic versus symmetric-top reorientation

Correlation times for both polysaccharides may be assumed to be similar, as they have similar molecular masses and ^{13}C R_1s. Correlation times for n.O.e. simulations for both polysaccharides were calculated by fitting to experimentally determined ^{13}C spin-lattice relaxation rates (R_1s) of **2**, as (a) its ^{13}C spectrum is particularly well resolved, allowing measurement of all ring

carbon R_1s; and (b) the IdoA ring in this compound can be considered as a simple $^1C_4$ chair conformation, as follows: it has been shown that 2-O-sulphated IdoA substituted at the 4-position with N-acetylglucosamine adopts the $^1C_4$ conformation in oligo-saccharides (van Boeckel et al., 1987a). Although measured $^3J_{H,H}$ values for **2** are not sufficiently accurate for an analysis of IdoA ring conformations, they are approximately similar to the values observed for the corresponding oligosaccharides studied by van Boeckel et al. (1987a). Those authors also noted that ^{13}C chemical shifts are sensitive to ring conformation, the $^2S_0$ conformation shifting resonances to low field. It is particularly noticeable that IdoA C^3 in **2** resonates at considerably higher field than IdoA C^3 in heparin (Table 2). The simplifying assumption was therefore

Table 5   Calculated low-energy glycosidic linkage conformations* in heparin (1) and de-N-desulphated re-N-acetylated heparin (2) disaccharides

Compound		Angle (°)		
		ϕ_H	ψ_H	$E†$
1(AI)‡	$^1C_4$	−30	−29	26
	$^2S_0$	−9	−41	32
2(AI)	$^1C_4$	−62	−41	27
	$^2S_0$	−24	−43	30
1(IA)	$^1C_4$	59	30	28
		−19	−33	28
	$^2S_0$	23	−56	29
		61	16	30
2(IA)	$^1C_4$	13	−48	26
		35	−12	27
	$^2S_0$	29	−52	29
		83	30	32

* MM2 minimized conformations from the lowest energy points found in the systematic search round the glycosidic linkages of **1** and **2**.

† Energy as calculated in the MM2 force field, expressed as kcal/mol (note: 1 kcal ≡ 4.184 kJ).

‡ I, iduronate; A, glucosamine.

(a) Isotropic rotor

(b) Symmetric top rotor

$\tau_\perp$
Slow

Fast
$\tau_\parallel$
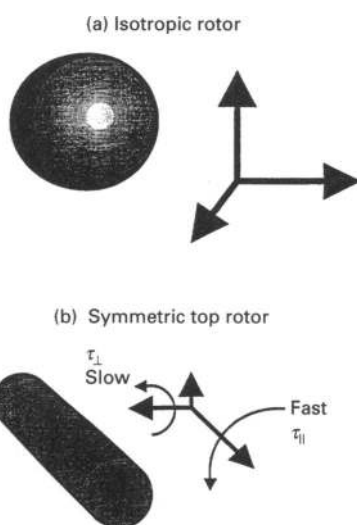
Figure 4   Two simple motional models of the reorientation in solution of macromolecules

The isotropic rotor (a) tumbles equally in all directions, with a motion characterized by a single relaxation time. The cylindrical symmetric top rotor (b) illustrated rotates more rapidly in one dimension than in the other two, and two correlation times are needed to characterize reorientation in solution: $\tau_\parallel$ for motion parallel with the main axis and $\tau_\perp$ for motion perpendicular to it.

made that the $^2S_0$ form for IdoA in **2** can be disregarded for the purpose of simulation of ^{13}C R_1s and $^1H-^1H$ n.O.e.s.

If an initial assumption of isotropic molecular reorientation in solution is made, and a correlation time chosen to give close agreement between simulated and experimental n.O.e.s for H^1-H^2

(a)   (b)
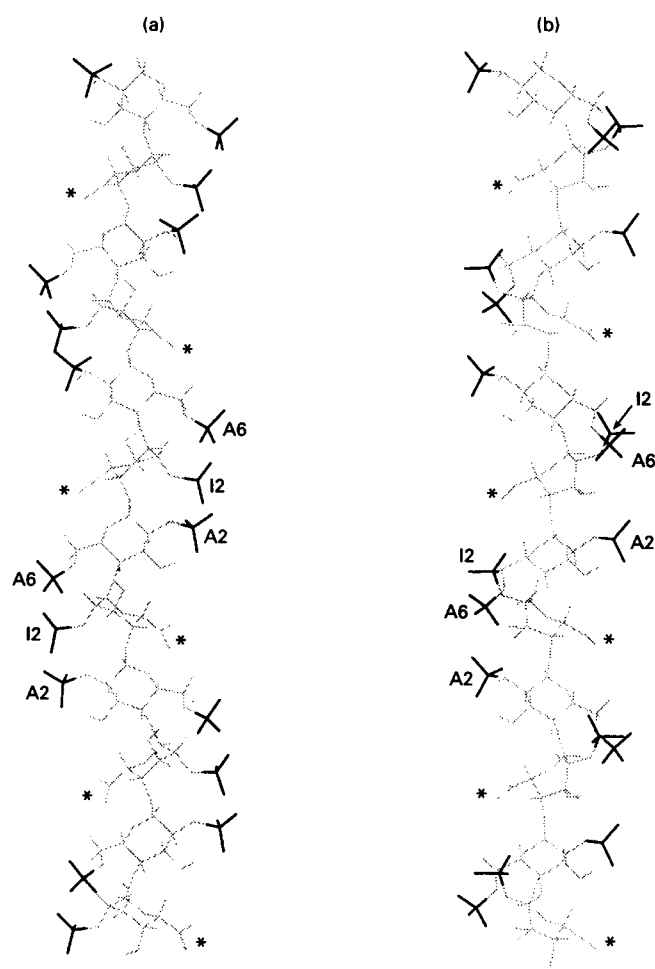
Figure 5   Diagrams of the solution conformations of (a) a heparin dodecasaccharide with the IdoA residue in the $^1C_4$ form and (b) a heparin dodecasaccharide with the IdoA residue in the $^2S_0$ form

Sulphate groups are shown in solid lines, with the residue and position labelled; asterisks indicate positions of carboxylate groups.

of the glucosamine residues, the magnitude of the n.O.e. for IdoA H^1-H^2 is consistently underestimated (by a factor of > 3 if the $^1C_4$ ring form is assumed; of about 2 if the $^2S_0$ form is assumed). No single correlation time could reconcile calculated and experimental n.O.e.s for both GlcN H^1-GlcN H^2 and IdoA H^1-IdoA H^2. The next simplest motional model is the symmetric top (Figure 4), which seems intuitively suitable for a linear molecule. It is possible to simulate n.O.e.s for this type of motion using NOEMOL, which will also calculate the orientations of the major and minor axes for a molecular model. The dodeca-saccharide models of **1** and **2** arising from energy calculations are linear helices, with the calculated major axis directly along the helix. In the symmetric top rotor, cross-relaxation rates depend on both the spin–spin distance and the angle between the spin–spin vector and the top axis. Consequently, $^1H-^1H$ interactions which lie perpendicular to the top axis give smaller n.O.e.s than those lying parallel to the main axis. Such a motional model has already been successfully used to simulate n.O.e.s for **2** (Forster et al., 1989).

By a process of trial and error, a value for $\tau_\perp$ of 8 ns and for $\tau_\parallel$ of 0.16 ns (implying rotation parallel to the major axis 50 times
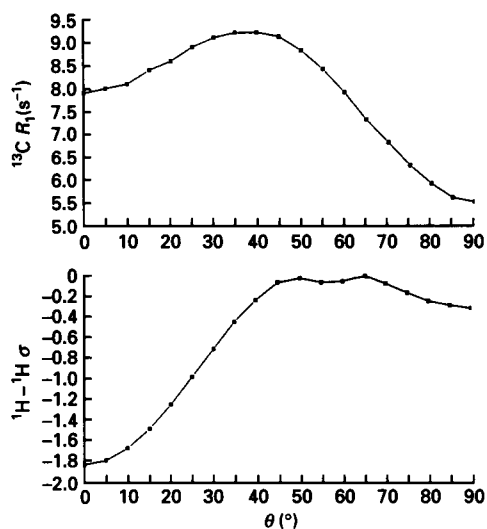
Figure 6   Plots of (a) ^{13}C R_1 at 50 MHz and (b) $^1H-^1H$ cross-relaxation rates [$\sigma(s^{-1})$] at 500 MHz against the angle θ between the C–H or H–H vector and the symmetric top axis using the correlation times $\tau_\perp = 8$ ns and $\tau_\parallel = 0.16$ ns

faster than rotation perpendicular to it) were found to give reasonable agreement between calculated and experimental ^{13}C R_1s at both 50 MHz and 67.5 MHz for 2 (Table 3).

n.O.e. simulations

As the major symmetric top axis runs centrally down the length of the helical model of 2, each disaccharide unit is equivalent with respect to angles made by corresponding C–H and H–H vectors with the top major axis. The ^1H and ^{13}C spectra of these polysaccharides consist of coincident contributions from each repeating disaccharide unit, so for n.O.e. simulations, irradiation of corresponding protons in each of several succeeding disaccharide units in the molecular model was simulated. Agreement between predicted and observed n.O.e.s for the model of 2 derived from conformational-energy calculations was good. Minor adjustments were made to the A–I linkage glycosidic torsional angles to improve the fit, and for the I–A linkage it became possible to rule out the low-energy conformation with ψ_H negative as a significant contributor to the equilibrium, because predicted H^1I-H^6A n.O.e.s were too small and H^1I-H^4A n.O.e.s too large to fit experimental values. A better fit was obtained with both ϕ_H and ψ_H at positive values, still well within the low-energy area of the maps in Figures 3(c) and 3(d). Comparisons of calculated and measured n.m.r. data for 2 are summarized in Table 3, and as the simulated n.O.e.s were found to be extremely sensitive to small alterations in inter-residue glycosidic angles, further small adjustments would have little physical significance.

For 1 the $^2S_0$ form of the IdoA ring must be taken into account, and the fit of simulated and experimental n.m.r. parameters becomes yet more approximate. Comparisons of calculated and measured n.m.r. data for 1 are listed in Table 4. The process of fitting $^1H-^1H$ n.O.e.s to a combination of two molecular models was accomplished by trial and error. However, n.O.e.s compatible with the experimental results could be pre-

dicted from models with glycosidic linkage conformations similar to those predicted on energy grounds alone, with alterations of torsional angles in the models of more than a few degrees seriously reducing the fit between experimental and observed n.O.e.s. ^{13}C R_1s were also reasonably well predicted (Table 4). As was the case for 2, the low-energy conformation for the I–A linkage in which ψ_H was negative could be ruled out as a major contributor. The final models of 1 are shown in Figure 5.

DISCUSSION

The interpretation of n.m.r. data presented here depends on several assumptions about the shapes and sizes of the molecules in solution. Use of the symmetric-top motional model implies that the relaxation phenomena governing $^1H-^1H$ n.O.e.s depend solely on correlation times determined by overall molecular reorientation of rigid, rod-like, molecules. A further implicit assumption has been made that the molecules in the n.m.r. sample are all the same size. The first of these assumptions is open to argument; the second is not justified, and the consequences of this should be examined.

Validity of the symmetric top model

Given the assumption that these molecules behave as rigid symmetric tops, ^{13}C R_1s should depend on the angles between C–H vectors and the top major axis. Unfortunately this relationship, which should provide a test of the validity of the symmetric-top motional model, is difficult to evaluate in these compounds. Fortuitously, the angles between C–H vectors and the top main axis for heparin and the modified heparins fall into a restricted range: between 60° and 80° for seven out of ten ring C–H vectors. Given the experimental errors in the measurement of R_1 values comparison of experimental and calculated ^{13}C R_1 values leads to no clear conclusions about the validity of the symmetric top model. On the whole, $^1H-^1H$ cross-relaxation rates depend much more strongly (about tenfold) on the angle between the spin–spin vector and the top main axis than do the ^{13}C R_1 values (about two-fold; see Figure 6).

The problem of polydispersity

The polysaccharides in this study are both polydisperse. Each sample will therefore contain molecules of a variety of different lengths and axial ratios and hence different values for $\tau_\perp$ and $\tau_\parallel$. Resonances in both ^1H and ^{13}C spectra will represent contributions from all the molecules in the sample, which for measurement of chemical shifts and coupling constants is not a problem. Interpretation of the experimental $^1H-^1H$ n.O.e.s and ^{13}C relaxation times is not as straightforward. For example, the R_1 value calculated by the inversion recovery method for these polydisperse samples is not related in any simple way to the individual relaxation rates of the superimposed carbon signals from each molecule. Treating the result as if it were a genuine R_1 is therefore not strictly justified.

Whatever is the relationship between measured values for $^1H-^1H$ n.O.e.s and ^{13}C R_1s and contributions to these from individual molecules in the sample, both are governed by the same correlation times; in the absence of a full theoretical treatment the approach adopted seems a reasonable expedient. The values used for $\tau_\perp$ and $\tau_\parallel$ are effective correlation times which account in an approximate fashion for a complex mixture of anisotropic overall reorientation and complex internal motions. We do not claim that the symmetric-top motional model is strictly valid for this class of compounds. Its use can only be

justified empirically as an aid to interpreting n.m.r. data in terms of three-dimensional molecular structures.

The molecular models of dodecasaccharides of heparin derived from the n.O.e. data as described above are shown in the $^1C_4$ form in Figure 5(a) and in the $^2S_0$ form in Figure 5(b). The overall length of each dodecasaccharide is near 5 nm (50 Å), implying a rise per residue of just over 0.4 nm (4 Å). These distances are similar for both the $^1C_4$ and $^2S_0$ conformations of the IdoA residues. The number of residues per turn is close to 4.

The model of heparin shown in Figure 5(a) is almost identical with the solid-state model of heparin derived from X-ray fibre diffraction measurements (Atkins and Nieduszynski, 1975; Nieduszynski et al., 1977). The crystallographic repeat unit was found to be a tetrasaccharide of length 1.65 nm (16.5 Å), close to the value of 1.67 nm (16.7 Å) given by our n.m.r. model. The best agreement with the diffraction data was given when IdoA was in the $^1C_4$ form and C^5–C^6 of the glucosamine residues in the g,g rotamer (Nieduszynski et al., 1977). Gatti et al. (1979) also provided some n.m.r. evidence that the solution structure of heparin resembles the solid-state structure; they found that the chemical shift of H^5 of the glucosamine residue was pH-sensitive, and attributed this to its close proximity to the carboxy group of the IdoA residue.

One distinctive feature of the structures shown in Figure 5 concerns the disposition of the sulphate substituents. In **1** three sulphates on successive residues form a cluster on one side of the polysaccharide chain (see Figure 5a for the model with IdoA in the $^1C_4$ form), the next three on the opposite side, and so on; the same clusters persist with an altered geometry when the iduronate residues take up the $^2S_0$ conformation (Figure 5b). Alteration of the orientation of the 2-O-sulphate of the IdoA residues is the most visible consequence of the change in ring conformation; the overall conformation of the chain is not greatly affected, as the optimal angles round inter-residue glycosidic linkages are similar for the $^1C_4$ and $^2S_0$ forms. Carboxylate groups of the IdoA residues are distributed about midway between the clusters of sulphates; their position is only slightly altered by the change in conformation of the iduronate ring. For **2**, ^{13}C shifts are consistent with published evidence that 2-O-sulphated IdoA residues in this type of sequence exist mainly in the $^1C_4$ form (van Boeckel et al., 1987a).

Representation of the conformational mobility of the IdoA ring as an equilibrium between the $^1C_4$ and $^2S_0$ forms may not reflect its full extent. In recent molecular-dynamics studies of unsulphated IdoA as the methyl glycoside and as the central residue in a trisaccharide (Forster and Mulloy, 1993), trajectories with $^2S_0$ as the initial ring form showed rapid pseudorotation between a range of different boat and skew-boat forms (rather than the small oscillations round a single form characteristic of trajectories starting with either of the two chair forms). There is so far, however, no experimental evidence for pseudorotational motion in IdoA residues in polysaccharides.

The rate of interchange of ring conformers of the iduronate residues in these compounds is not sufficiently rapid to affect ^{13}C R_1s (or the amplitude of the resulting motion of the CH vectors is sufficiently small that ^{13}C R_1s are not greatly affected). It is, however, rapid enough to average ^{13}C chemical shifts; perhaps in the range 10^4–10^6 Hz.

Characterization of heparin as a helix bearing linear arrays of sulphate clusters has implications for the nature of the heparin-binding sites of proteins. Whereas in the highly sequence-specific interaction of heparin with antithrombin other groups, such as carboxylates, play a necessary role (van Boeckel et al., 1987b), less specific ionic interactions between heparin and proteins will be dominated by the highly acidic sulphate groups, at least in

fully sulphated sequences (i.e. **1**). Cardin et al. (1991) have identified a peptide of apolipoprotein E which adopts an α-helical conformation on binding to heparin; the amphipathic helix has one hydrophobic face and a positively charged face suitable for binding to a parallel heparin helix. Similar helical structures have been predicted for heparin-binding sites in a number of proteins (Cardin and Weintraub, 1989); within these sequences, basic residues occur in clusters of two or three. Ferran et al. (1992) have designed and synthesized a helical heparin-binding peptide with cationic residues spaced so that their positively charged side chains are on one face of the helix; Pratt and Church (1992) have identified a peptide from protein C inhibitor which has these properties and binds heparin, and showed that the same residues in random order do not have the same affinity for heparin. The induction of helical secondary structure in basic homopolypeptides by binding to heparin has long been recognized (Blackwell et al., 1977). Other interactions between heparin and proteins involve only a small part of the heparin molecule; these include the capacity of heparin to compete with $Ins(1,4,5)P_3$ for its receptor (Tones et al., 1989); and probably the important interaction between heparin and growth factors; sulphated sugars as small as disaccharides can mimic the stabilizing and potentiating function of heparin with basic fibroblast growth factor (Folkman and Shing, 1992). The importance of the mobility of the IdoA ring in heparin–protein interactions has not yet been defined, but it must affect systems on this scale where the precise orientation of sulphate groups is vital.

REFERENCES

Allen, F. H., Kennard, O., Watson, D. G., Brammer, L., Orpen, A. G. and Taylor, R., (1987) J. Chem. Soc. Perkin Trans. II, S1–S15

Atkins, E. D. T. A. and Nieduszynski, I. A. (1975) Adv. Exp. Med. Biol. **52**, 19–37

Bangham, D. R. and Mussett, M. V. (1959) Bull. WHO **20**, 1201–1208

Blackwell, J., Schodt, K. P. and Gellman, R. A. (1977) Fed. Proc. Fed. Am. Soc. Exp. Biol. **36**, 98–101

Burkert, U. and Allinger, N. (1982) ACS Monogr. **177**

Cardin, A. D. and Weintraub, H. J. R. (1989) Arteriosclerosis **9**, 21–32

Cardin, A. D., Demeter, D. A., Weintraub, H. J. R. and Jackson, R. L. (1991) Methods Enzymol. **203**, 556–583

Chamberlain, L. N., Edwards, I. A. S., Stadler, H. P., Buchanan, J. G. and Thomas, W. A. (1981) Carbohydr. Res. **90**, 131–137

Cowan, S. W., Bakshi, E. N., Machin, K. J. and Isaac, N. W. (1986) Biochem. J. **234**, 485–488

Damon, D. H., Lobb, R. R., D'Amore, P. A. and Wagner, J. A. (1989) J. Cell Physiol. **138**, 221–226

Danishevsky, I., Eiber, H. B. and Carr, J. J. (1960) Arch. Biochem. Biophys. **90**, 114–121

Ferran, D. S., Sobel, M. and Harris, R. B. (1992) Biochemistry **31**, 5010–5016

Ferro, D. R., Provasoli, A., Ragazzi, M., Torri, G., Casu, B., Gatti, G., Jacquinet, J.-C., Sinäy, P., Petitou, M. and Choay, J. (1986) J. Am. Chem. Soc. **108**, 6773–6778

Ferro, D. R., Provasoli, A., Ragazzi, M., Casu, B., Torri, G., Bossennec, V., Perly, B., Sinäy, P., Petitou, M. and Choay, J. (1990) Carbohydr. Res. **195**, 157–167

Folkman, J. and Shing, Y. (1992) Adv. Exp. Med. Biol. **313**, 355–364

Forster, M. J. and Mulloy, B. (1993) Biopolymers **33**, 575–588

Forster, M. J., Jones, C. and Mulloy, B. (1989) J. Mol. Graph. **7**, 196–201

French, A. D. (1988) Biopolymers **27**, 1519–1525

Gospodaröwicz, D. and Cheng, J. (1986) J. Cell. Physiol. **128**, 475–484

Hore, P. J. (1983) J. Magn. Reson. **54**, 539–542

Gatti, G., Casu, B., Hamer, G. K. and Perlin, A. S. (1979) Macromolecules **12**, 1001–1007

Grootenhuis, P. D. J. and van Boeckel, C. A. A. (1991) J. Am. Chem. Soc. **113**, 2743–2747

Jeffrey, G. A. and Taylor, R. (1980) J. Comput. Chem. **1**, 99–109

Johnson, E. A. J. and Mulloy, B. (1976) Carbohydr. Res. **51**, 119–127

Lamba, D., Mackie, W., Sheldrick, B., Belton, P. and Tanner, S. (1988) Carbohydr. Res. **180**, 183–193

Mitra, A. K., Arnott, S., Atkins, E. D. T. and Isaac, D. H. (1983) J. Mol. Biol. **169**, 873–901

Nagasawa, K. and Inoue, Y. (1980) Methods Carbohydr. Chem. **8**, 287–289

Nieduszynski, I. A., Gardner, K. H. and Atkins, E. D. T. (1977) Am. Chem. Soc. Symp. Ser. **48**, 73–80

Nishida, Y., Hori, H., Ohrui, H. and Meguro, H. (1988) J. Carbohydr. Chem. **7**, 239–250

Pratt, C. W. and Church, F. C. (1992) J. Biol. Chem. **267**, 8789–8794

Ragazzi, M., Ferro, D. R. and Provasoli, A. (1986) J. Comput. Chem. **7**, 105–112

Ragazzi, M., Ferro, D. R., Perly, B., Sinaÿ, P., Petitou, M. and Choay, J. (1990) Carbohydr. Res. **195**, 169–185

Rao, B. N. N., Dua, V. K. and Bush, C. A. (1985) Biopolymers **24**, 2207–2229

Rapraeger, A. C., Krufka, A. and Olwin, B. B. (1991) Science **252**, 1705–1708

Sanderson, P. N., Huckerby, T. N. and Nieduszynski, I. A. (1987) Biochem. J. **243**, 175–181

Savitsky, D., Hampl, H. and Habermehl, K.-O. (1990) J. Gen. Virol. **71**, 1221–1225

Tones, M. A., Bootman, M. D., Higgins, B. F., Lane, D. A., Pay, G. F. and Lindahl, U. (1989) FEBS Lett. **252**, 105–108

van Boeckel, C. A. A., van Aelst, S. F., Wagenaars, G. N., Mellema, J.-R., Paulsen, H., Peters, T., Pollex, A. and Sinnwell, V. (1987a) Recl. Trav. Chim. Pays-Bas **106**, 19–29

van Boeckel, C. A. A., Lucas, H., van Aelst, S. F., van den Nieuwenhof, M. W. P., Wagenaars, G. N. and Mellema, J.-R. (1987b) Recl. Trav. Chim. Pays-Bas **106**, 581–591

Yayon, A., Klagsbrun, M., Esko, J. D., Leder, P. and Ornitz, D. M. (1991) Cell **64**, 841–849